Published in final edited form as:
J Am Chem Soc. 2009 March 18; 131(10): 3438–3439. doi:10.1021/ja809227c.

Transmembrane structures of amyloid precursor protein dimer predicted by replica-exchange molecular dynamics simulations

Naoyuki Miyashita[†], **John E. Straub**[‡], **D. Thirumalai**[§], and **Yuji Sugita**[¶,*]

[†] RIKEN Computational Science Research Program, Molecular Scale Team, 2-1 Hirosawa, Wako, Saitama 351-0198, Japan

[‡] Boston University, Department of Chemistry, 590 Commonwealth Ave. Boston, Massachusetts 02215-2521

[§] Department of Chemistry and Biochemistry and Biophysics Program, Institute for Physical Science and Technology, University of Maryland, College Park, Maryland 20742

[¶] RIKEN Advanced Science Institute, 2-1 Hirosawa, Wako, Saitama 351-0198, Japan

Aggregation of amyloid β peptide (Aβ) in the brain is the primary element in the pathogenesis of Alzheimer's disease (AD).[1] Aβ is produced from amyloid precursor protein (APP), which is a type I transmembrane (TM) glycoprotein in neural and non-neural cells. APP is first cleaved on the β-site by β-secretase, and the extracellular domain of APP is dissociated from the remaining protein (APP-C99). γ-secretase then cleaves the γ-site (Gly_{38}-Thr_{43}), which is located on the TM domain of APP-C99. Finally, Aβ is released to the extracellular region. Because the γ-site contains several cleavage points (see supporting figure 1), Aβ of different chain lengths are observed. Of these, $Aβ_{1-40}$ and $Aβ_{1-42}$ are primary and secondary isoforms, respectively.

Structural information on Aβ and its aggregated forms has been accumulated by NMR spectroscopy and X-ray crystallography.[2] A number of molecular dynamics (MD) simulations on the aggregation of Aβ in solution have also been performed.[3] In contrast, little is known about the TM structures of APP/APP-C99. Since the amyloid accumulation depends on the chain length of Aβ, it is relevant to understand how Aβ is cleaved by γ-secretase and released from APP-C99. To address this key question, we have determined the monomer structure of APP-C99 fragment ($Aβ_{1-55}$), which has two α-helical regions from His_{13} to Val_{18} and from Ala_{30} to Lys_{53} by replica-exchange molecular dynamics (REMD) simulations.[4]

APP/APP-C99 contains three Gly-XXX-Gly motifs in TM and juxtamembrane (JM) regions. The motif is known to promote dimerization of polypeptides via $C_α$-H…O hydrogen bonds between two segments in a membrane environment. A pairwise replacement of Gly (Gly_{29} and Gly_{33}) with Leu (Leu_{29} and Leu_{33}) in APP enhances the homo dimerization, but leads to a drastic reduction of $Aβ_{1-40}$ and $Aβ_{1-42}$ secretion.[5] To resolve this apparent discrepancy, it would be useful to predict the homo-dimer conformation of APP/APP-C99 in the membrane. Understanding the homodimer conformation of APP/APP-C99 is essential for elucidating the last step in the formation of Aβ associated Alzheimer's disease.

sugita@riken.jp.

Supporting Information Available: The supporting methods and figures are available free of charge via the Internet at (http://pubs.acs.org/paragonplus/submission/jacsat/).

We performed REMD simulations of two APP fragments ($A\beta_{23\text{-}55}$) in a membrane environment for both the wild type (WT) sequence and a mutant, in which Gly_{29} and Gly_{33} are replaced with Leu_{29} and Leu_{33}. MMTSB toolsets with the CHARMM 19 EEF1.1 force field were used for the calculations[6] (the simulation details are given in the supporting materials). The effects of solvent and membrane on the APP fragments were included implicitly in IMM1 model.[7]

At 300 K, secondary and tertiary structures of the mutant APP fragments differ from those of the WT. In figure 1, we compare α-helicity of each residue in the WT with that in the mutant. The similarity of α-helicity in the top (colored in red) and bottom (in green) plots indicates that the REMD simulations were able to sample all the possible configurations of the APP fragments in the membrane. Marked contrasts in the α-helicity between the WT and the mutant are observed in residues 29–38. This region was observed to be unwound in the WT, whereas it formed an α-helix in the mutant. In figure 2, Leu_{29} in the mutant was located in the membrane, whereas Gly_{29} in the WT was in the extracellular region. The position of Leu_{49} was not altered by the mutation. Each mutant APP fragment was, therefore, more tilted (see supporting figure 3). As a result, the γ-site in the mutant was shifted toward the center of the membrane.

We also investigated the homo-dimer conformations of the WT and the mutant APP fragments at 300 K by principal component analysis (PCA)[9] of the backbone atoms in the region from Gly_{29} to Thr_{43}. By using the first and third principal components (PC1 and PC3), we obtained two major peaks for the mutant (PM1: 65.4%, PM2: 28.5%) and several other peaks for the WT fragments (see supporting figure 4). Because of the backbone flexibility observed in the WT, PCA could not classify major dimer structures. Instead, we used C_α-H…O hydrogen bonds between two fragments for these classifications as shown in supporting figure 5.

We observed three different types of the homo-dimer conformation of APP fragments in the membrane. The first type observed only in the WT, was stabilized by C_α-H…O hydrogen bonds between the two APP fragments. These bonds are the most characteristic interaction between two fragments that contain Gly-XXX-Gly motifs. Due to the three Gly-XXX-Gly motifs in the WT APP fragments, multiple C_α-H…O hydrogen bonds were observed. Of these, the hydrogen bonds involving Gly_{33} and Gly_{38} were essential for the dimerization of the WT APP fragments (figure 3a inset and supporting figure 6). This causes a partial unwinding of α-helix in the residues 29–38 as shown in figure 1. Solid-state NMR spectroscopy has also shown that the glycines in the Gly-XXX-Gly motif line at the dimer interface.[10]

In the second type of dimer conformation, hydrophobic residues intervened between two APP fragments. This conformation was observed mainly in the mutant (PM1 in figure 3), because the mutated Leu_{29} and Leu_{33} contributed significantly. In addition to the mutated residues, Ile_{31}, Leu_{34}, or Val_{36} intervened between two APP fragments. Therefore, this form was also observed in the WT as a minor conformation. In contrast, in the third type of dimer conformation two APP fragments crossed with each other at Gly_{38}. This conformation is similar to the conformation of glycophorin A, which also has a Gly-XXX-Gly motif in the TM region.[11] This conformation populated roughly 28.5% (in PM2) in the mutant, whereas it represented less than 1.0 % in the WT. The Gly-rich region of the TM and JM regions in the WT would be too flexible to take on this conformation.

How do the conformational differences between the WT and the mutant affect the secretion of Aβ or the cleavage by γ-secretase? As shown in figure 2, the γ-site (Gly_{38}-Thr_{43}) in the mutant is shifted downward about 3 Å along the bilayer normal. In addition, the conformational flexibility of the γ-site might be increased in the mutant, because of the lack of inter-fragment C_α-H…O hydrogen bonds at Gly_{38}. These changes likely induce mismatched interactions

between the γ-site of APP-C99 and the active site of γ-secretase, which would reduce the secretion of $A\beta_{1\text{-}42}$ or $A\beta_{1\text{-}42}$.[5]

In summary, we have predicted the APP ($A\beta_{23\text{-}55}$) fragment dimer structures of the WT and a mutant protein using REMD simulations and found drastic changes of dimer structures by the mutation.[5] The results are in good agreement with the existing experimental data[5,10] and provide fundamental insight into the initial steps in the amyloid formation.

Supplementary Material

Refer to Web version on PubMed Central for supplementary material.

Acknowledgments

This research was supported in part by a Grant for Scientific Research on a Priority Areas 'Membrane Interface' (to YS) and the Development and Use of the Next-Generation Supercomputer Project of the Ministry of Education Culture, Sports, Science and Technology (MEXT), and by CREST & BIRD, Japan Science and Technology Agency (JST) (to YS). DT and JES are thankful for the support of a grant from the national institute of health (RO1 GM076688-05). We thank the RIKEN Super Combined Cluster (RSCC) for providing computational resources.

References

1. See for instance, Haass C, Selkoe DJ. Nature Reviews Molecular Cell Biology 2007;8:101–112.112
2. See for instance, (a)Petkova AT, Yau WM, Tycko R. Biochemistry 2006;45:498–512.512 [PubMed: 16401079](b)Nelson R, Eisenberg D. Curr Opin Struc Biol 2006;16:260–265.265
3. There are number of papers. See for ex., (a)Tarus B, Straub JE, Thirumalai D. J Am Chem Soc 2006;128:16159–16168.16168 [PubMed: 17165769](b)Tarus B, Straub JE, Thirumalai D. J Mol Biol 2005;345:1141–1156.1156 [PubMed: 15644211](c)Massi F, Peng JW, Lee JP, Straub JE. Biophys J 2001;80:31–44.44 [PubMed: 11159381]
4. (a) Sugita Y, Okamoto Y. Chem Phys Lett 1999;314:141–151. (b) Miyashita N, Straub JE, Thirumalai D. to be published
5. Kienlen-Campard P, Tasiaux B, Hees JV, Li M, Huysseune S, Sato T, Fei JZ, Aimoto S, Courtoy PJ, Smith SO, Constantinescu SN, Octave JN. J Biol Chem 2008;283:7733–7744. [PubMed: 18201969]
6. (a) Feig M, Karanicolas J, Brooks CL. J Mol Graphics and Modeling 2004;22:377–395. (b) MacKerell AD Jr, et al. J Phys Chem B 1998;102:3586–3616.
7. Lazaridis T. Proteins 2003;52:176–192. [PubMed: 12833542]
8. Kabsch W, Sander C. Biopolymers 1983;22:2577–2637. [PubMed: 6667333]
9. (a) Kitao A, Go N. Curr Opin Struc Biol 1999;9:164–169. (b) García AE. Phys Rev Lett 1992;68:2696–2699. [PubMed: 10045464]
10. Sato T, Tang T, Reubins G, Fei JZ, Fujimoto T, Kienlen-Campard P, Constantinescu SN, Octave JN, Aimoto S, Smith SO. Proc Natl Acad Sci USA 2009;106:1421–1426. [PubMed: 19164538]
11. (a) MacKenzie RA, Prestegard JH, Engelman DM. Science 1997;276:131–133. [PubMed: 9082985] (b) Senes A, Ubarretxena-Belandia I, Engelman DM. Proc Natl Acad Sci USA 2001;98:9056–9061. [PubMed: 11481472]

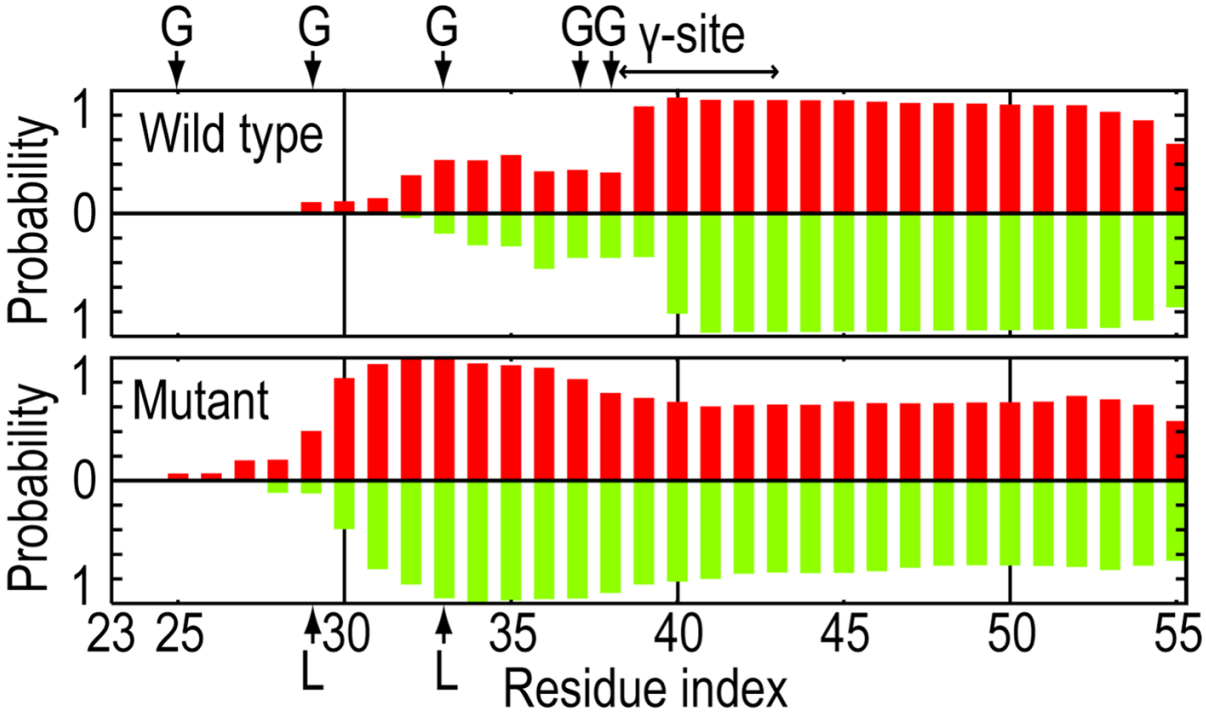

Figure 1.

α-helical content of each residue in the wild type (a) and the mutant (b) proteins at 300 K. The α-helical residue is defined with DSSP.[8] Green and red lines represent the α-helical content for two fragments in WT and the mutant. The locations of Gly, mutated Leu, and the γ-site are explicitly shown.

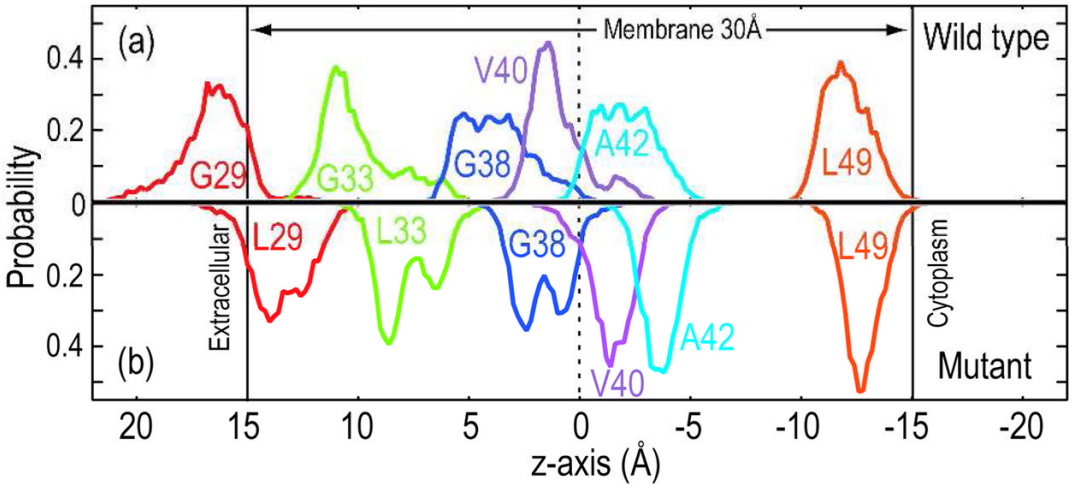

Figure 2.
The distributions of the Cα positions of G29 and L29 (red), G33 and L33 (green), G38 (blue), V40 (purple), A42 (cyan), and L49 (orange) along the z-axis for the WT (a) and the mutant (b) proteins.

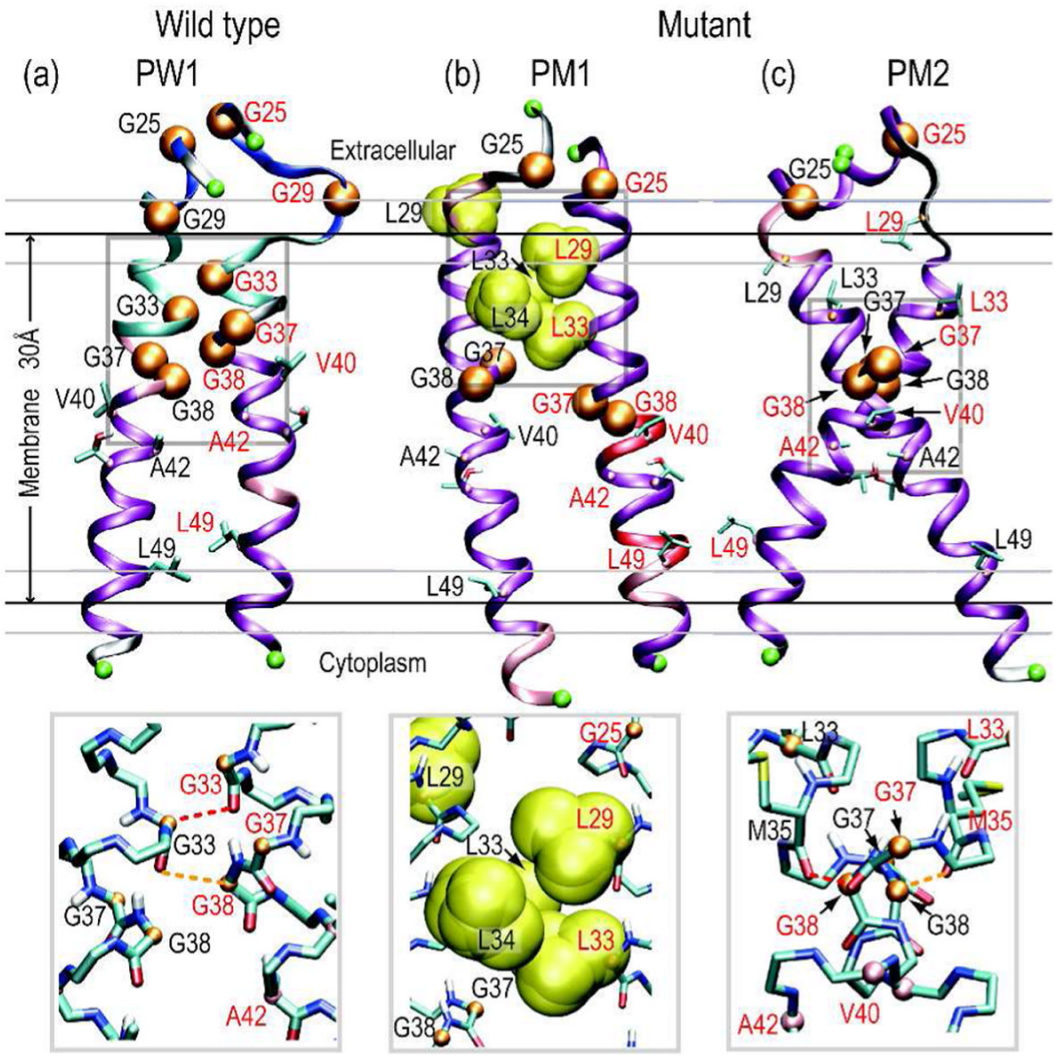

Figure 3.

Structures of major dimer conformations of the WT (a), and the mutant (b and c). Gray boxes indicate specific dimerization sites, and are enlarged at the bottom. Red and orange dashes indicate strong and medium C_α-H…O hydrogen bonds, respectively.